Available online at www.sciencedirect.com
SCIENCE DIRECT®
Polymer 44 (2003) 6033–6042
polymer
www.elsevier.com/locate/polymer

Process–structure–property relationships of erodable polymeric biomaterials: II—long range order in poly(desaminotyrosyl arylates)

Michael Jaffe[a,*], Zohar Ophir[a], George Collins[a], Ali Recber[a], Seung-uk Yoo[a], Joseph J. Rafalko[b]

[a]*Medical Device Concept Laboratory, Department of Biomedical Engineering, New Jersey Institute of Technology, 111 Lock Street, Newark, NJ 07103, USA*
[b]*Ticona Inc., 86 Morris Avenue, Summit, NJ 07901, USA*

Received 8 April 2003; received in revised form 17 June 2003; accepted 17 June 2003

Dedicated to Prof. Ian M. Ward on the occasion of his 75th birthday

Abstract

The long-range order of some bioerodable polyesteramides based on a desaminotyrosyl [Thermochim Acta 396 (2003) 141; Polym Adv Technol 13 (2002) 926; J Am Chem Soc 119 (1997) 4553] diol monomer has been investigated. The order is mesogenic, best described as a 'condis crystal' or smectic-like. In all cases where long-range order is present, ordered H bonds between amide groups are observed. The order stabilizes the polymer to dimensional change and mechanical relaxation under biorelevant conditions.

Keywords: Mesogenic bioerodable polyesteramide; FT-IR; Hydrogen bonding

1. Introduction

In recent years, a broad range of synthetic, bioerodable polymers have been investigated as tissue engineering scaffolds or as materials to enable a variety of biomedical devices [1,2]. This literature is replete in papers dealing with the effects of various polymer chemistries and macro-architectures on cellular response but little work has been done to define the impact of polymer processing or morphology on the performance of these materials either with respect to cellular interactions or rate of property decay in vivo. Jaffe [3,4] has initiated a series of studies to define the impact of morphology and molecular orientation on the mechanical properties, dimensional stability, bioerosion rates and biological activity of erodable polymeric biomaterials. Current studies are focussed on the combinatorial library of Desaminotyrosinetyrosyl (DT) containing polyarylates synthesized by Kohn [5,6]. The chemistry of the library matrix is shown in Fig. 1, while Fig. 2 shows a typical published library property, dry T_g, as a function of polymer molecular structure. Recently, Jaffe et al. [4] has shown these polymers to be unexpectedly richly structured, describing long-range order in compositions with aliphatic length in sidechain and diacid of at least eight $(CH)_2$ units, leading to the retention of process induced morphology under biorelevant conditions (aqueous, 37 °C), even though 37 °C is significantly higher than the reported T_g [5]. In contrast, it has been shown that plasticization by water causes significant shrinkage and mechanical property loss (molecular relaxation) in molecularly oriented fibers of the short side-chain and short diacid variants of the poly(DTR,Y) library under similar conditions, although the reported dry T_g's are significantly above 37 °C [6]. These results demonstrate the importance of morphology, and chain interactions on biorelevance performance.

In this paper, the aspects of the novel long-range order observed in some compositions of the poly(DTR,Y) combinatorial library are examined by temperature and time dependent Fourier transform infra-red spectroscopy (FTIR), hot stage optical microscopy (OM) and thermally stimulated current analysis (TSC). The observed mesogenic order is clearly associated with the formation of ordered H bonds through the backbone amide linkage. Results are discussed in terms of the formation of the observed mesophases as well as the implications of the structure to in vivo polymer utility.

* Corresponding author.
E-mail address: jaffe@adm.njit.edu (M. Jaffe).

0032-3861/03/$ - see front matter © 2003 Elsevier Ltd. All rights reserved.
doi:10.1016/S0032-3861(03)00559-7

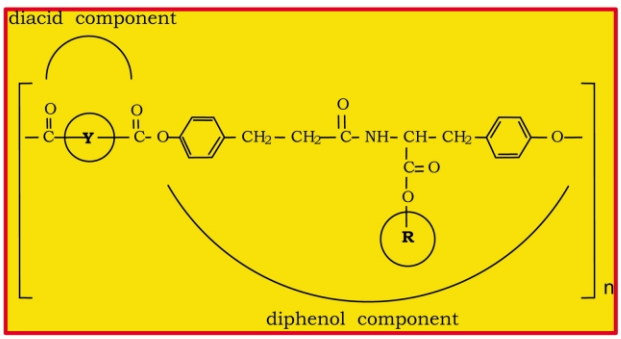

- Nomenclature (R,Y) = length of alkane in sidechain, backbone

Fig. 1. DesAmino tyrosyl polymers. Nomenclature (R,Y) = length of alkane in sidechain, backbone.

2. Experimental

Samples of the poly(DT2,2), poly(DT2,10), poly(DT8,8) and poly(DT12,10) were synthesized in the laboratories of Advanced Material Design Co., and supplied as powders of specified molecular weights in quantities ranging from 50 to several hundred grams. Fiber and film samples were fabricated by Jaffe and characterized by a variety of thermal analysis techniques as previously described [3,4].

Infrared spectra were obtained using a Harrick single pass horizontal ZnSe ATR crystal with a 45° angle. The temperature was controlled by a heated clamped aluminum block that sandwiched the sample between the block and the ATR crystal. An Omega 2011 controller was used to control the heating. Heating rates were nominally 5 °C/min between 30 and 75°. Above this temperature, the rate slowed appreciably, as the heating element was not capable of handling the load. Cooling experiments were run by turning off the heater and observing the cooling of the sample. Naturally, the cooling rates were faster from higher temperatures. Even with the heating and cooling rate variations, sharp, distinct transitions were observed at transition temperatures by monitoring rapid intensity changes in the total infrared spectrum or at specific frequencies. The transition temperatures measured by this technique were within a few degrees of those determined by DSC. Data were not collected for the first heating because this cycle was used to establish intimate contact of the sample with the crystal that could not be accomplished by pressure alone.

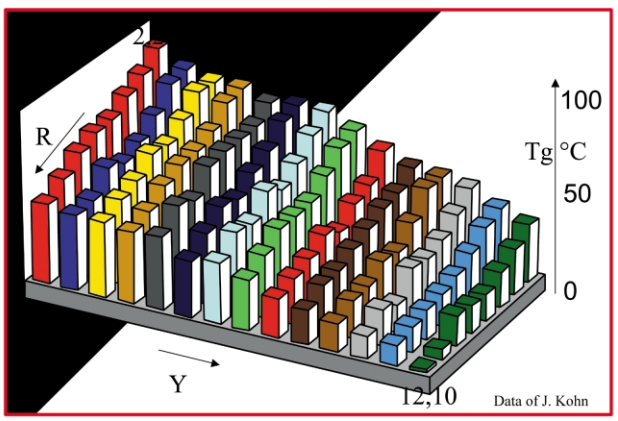

Fig. 2. Glass transition temperature as a function of polymer structure.

A Digilab FTS 6000 with an MCT detector operating in kinetics mode was used to acquire the 4 cm^{-1} infrared spectra. A 10 s time resolution was utilized. Fifty scans were obtained in this time frame.

Texture micrographs of the polymer were obtained with a ZEISS polarized optical microscope fitted with a 35 mm camera back. Pieces of poly(DT12,10) film, 0.5 cm × 0.5 cm × 0.15–0.20 mm thick, were lightly pressed with a glass slide at room temperature. The sample was put onto a fresh glass slide and covered with cover glass with 1–2 drops of Type B mounting fluid. The sample was observed between crossed polars at room temperature at a total magnification of 400 × .

Thermally stimulated polarization current experiments (TSPC) were performed using a TherMold TSC/RMA 9000 instrument. A film specimen of the poly(DT12,10), 0.393 mm thick, was placed between stainless steel electrodes. The effective diameter of the electrodes was 6.85 mm. An electric field of 100 V/mm was imposed across the specimen as it was heated at 7 °C/min from 0 to 90 °C in a 1.1 bar dry helium environment. The specimen was monitored for polarization current over the entire range of the linear heating ramp. The lower limit of the current measurement was 10^{-16}–10^{-15} A.

3. Results and discussion

It has been previously shown that poly(DT8,8) and poly(DT12,10) exhibit endothermic processes upon heating and, in the case of poly(DT12,10) an exothermic event upon cooling. A typical DSC trace for the poly(DT12,10) is shown in Fig. 3, showing a number of endothermic events upon heating and a single exothermic event on cooling. Note the heat of transition of 23 J/g on cooling is indicative of

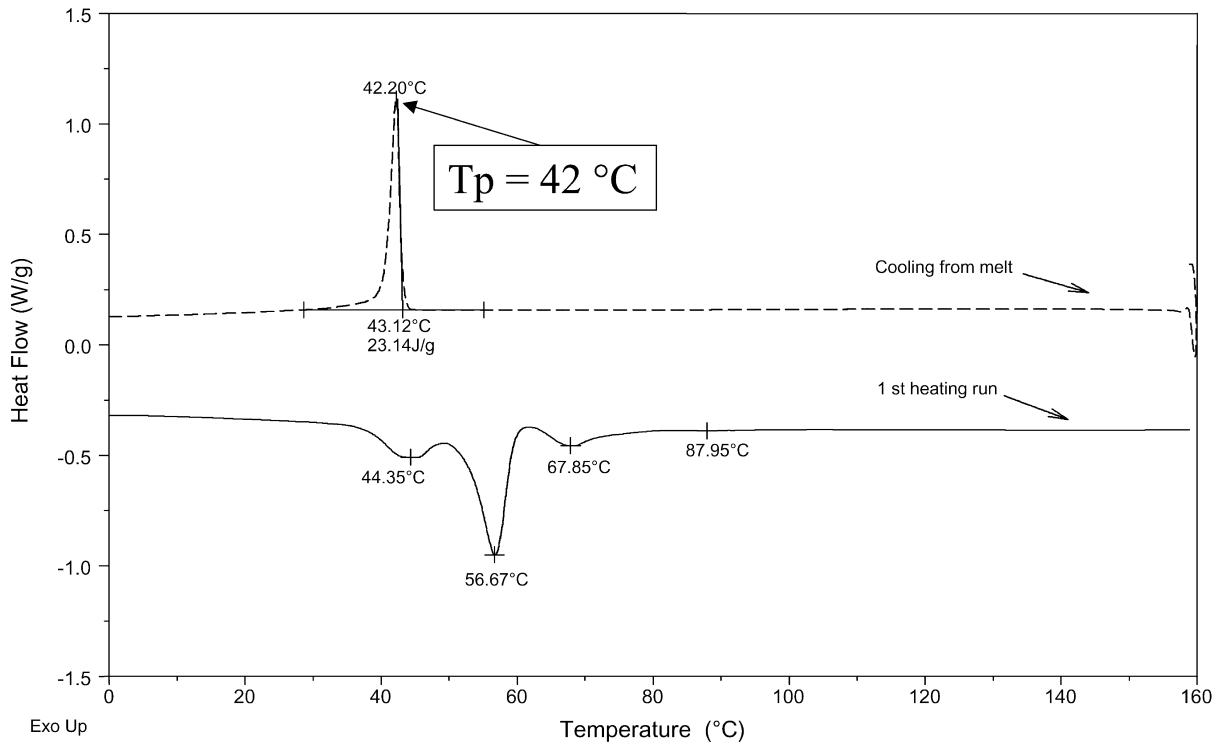

Fig. 3. Poly(DT12,10) heating and cooling.

either a semi-crystalline or a mesogenic phase transition but is significantly higher than the ~6 J/g noted in the 'melting' of thermotropic nematic polyesters [7]. Jaffe [3,4] has characterized these materials as 'condis crystals' [8,9] and noted that they possess many of the properties of the smectic-phase in polymers, i.e. they possess a highly layered structure. Fig. 4 shows that a smectic-like mesogenic texture is obtained between crossed polars with sheared samples of molecularly oriented poly(DT12,10). Unsheared samples show little texture other than orientation induced birefringence and the texture induced by shearing the sample relaxes away over a period of days. The lack of clear mesogenic textures in samples viewed between crossed polars is consistent with the 'condis' designation [8,9] that also often possesses smectic-like layered ordering. This is consistent with the wide angle X-ray diffraction pattern of this sample shown in Fig. 5a, which shows a single intense spacing along the meridian, corresponding to about 2.7 nm (the distance between side chains along the molecular backbone), and only a nearest neighbor spacing of about 4 Å on the equator. In contrast, the wide angle X-ray diffraction pattern of an oriented sample of the poly(DT2,2), Fig. 5(b), shows only the nearest neighbor spacing (amorphous halo) with increased intensity on the equator. The poly(DT2,2) and the poly(DT2,10) are amorphous polymers characterized only by a glass transition and, at least in the case of the poly(DT2,2), the structure is highly plasticized by water as illustrated in the DSC traces of the glass transition shown in Fig. 6 [3,4], leading to the loss of process induced properties under in vivo use conditions. Hence, while the description of the phase nature of the poly(DT12,10) and poly(DT8,8) is elusive, the resulting stability of induced molecular orientation exhibited by these structured polymers during in vivo use conditions is clearly evidenced by the retention of mechanical properties and heightened dimensional stability.

Thermally stimulated polarization current (TSPC) is a thermal analysis technique that follows the temperature dependent current generated as a consequence of molecular scale motion of dipoles. In a typical experiment, a voltage is applied across a test specimen and the temperature is increased using a linear program. When there is sufficient internal energy for molecule motion, the dipoles of the molecular framework will orient to the field. Fig. 7 shows the TSPC profile of the poly(DT12,10) polymer.

As the temperature is increased the motion of the charged structures in poly(DT12,10) generate a profile that is qualitatively similar to what is observed for this material in DSC experiments (Fig. 3). There are three distinct events at about 25, 42 and 62 °C. While more work will be required with this material to clarify its TSPC behavior, it appears in Fig. 7 that the peak at 62 °C has the sharp features of the enthalpic reordering that is consistent with a melting or a mesogenic transition. The two lower temperature peaks have the smooth contours that are suggestive of structural relaxation, suggestive of sub-glass transition or conformational disordering relaxation processes. It has been noted by Jaffe [3,4] that annealing both sharpens and increases the temperature of the largest of the phase change endotherms

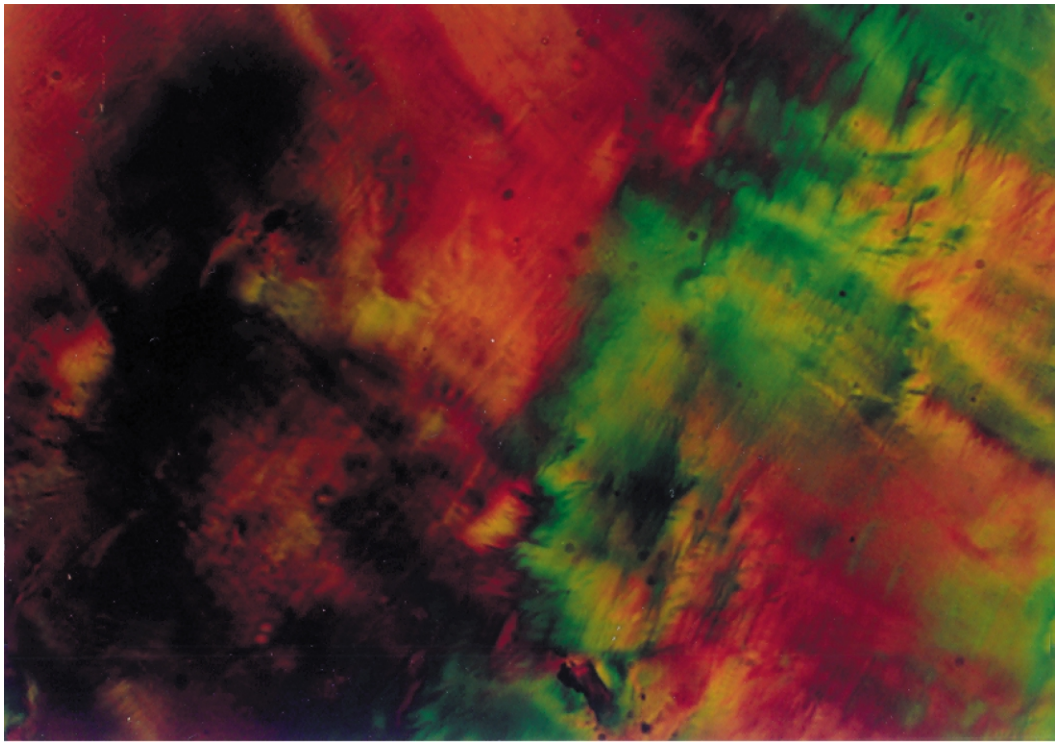

Fig. 4. Poly(DT12,10). Optical micrograph—crossed polars—room temperature.

noted on heating but that the lower temperature events also are preserved. These results imply that the thermally induced chain packing reorganizations that occur in the poly(DT12,10) as a function of process history involve dipole relaxation of a variety of types, consistent with mesogenic polymer structures.

The room temperature infrared carbonyl band structures of the four polymers studied are displayed in Fig. 8. They are very similar within each group, i.e. the poly(DT8,8) and the poly(DT12,10) constitute one group with the poly(DT2,2) and the poly(DT2,10) forming a second group, but are significantly different between the two sets of polymers. The spectra of the amorphous polymers have two amide bands near 1680 and 1652 cm^{-1} that can be attributed to free (non-hydrogen bonded) amide carbonyl groups and disordered hydrogen bonded carbonyl groups, respectively. These two conformations are typical of amorphous polyamides [10]. A third band related to ordered hydrogen bonded carbonyls is expected in spectra of ordered polymers at a slightly lower frequency than that found for the disordered hydrogen bonded carbonyl groups [11]. The spectra of the poly(DT12,10) and poly(DT8,8)

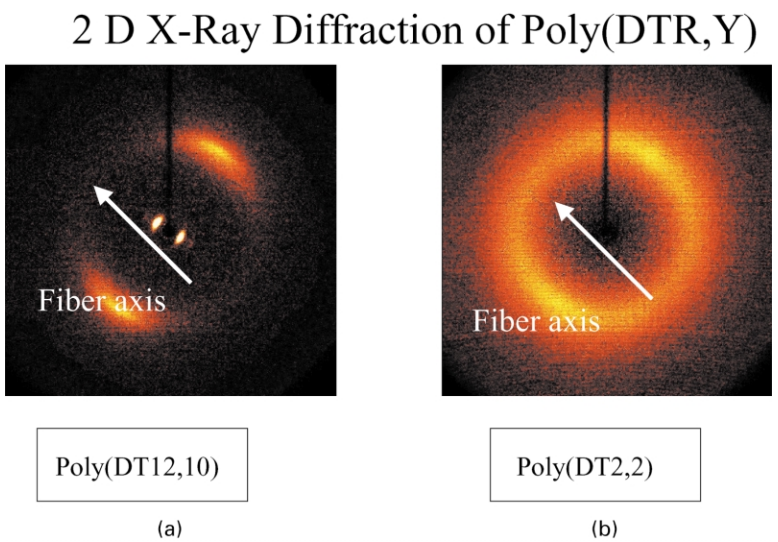

Fig. 5. 2D X-ray diffraction of poly(DTR,Y). (a) Poly(DT12,10); (b) poly(DT2,2).

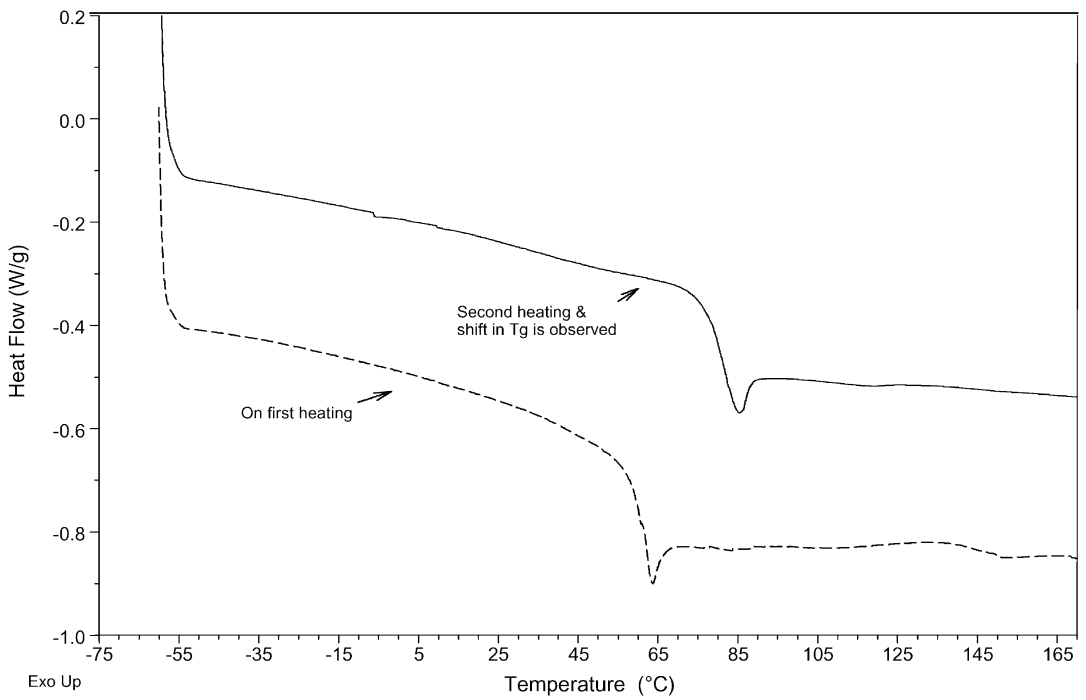

Fig. 6. Glass transition of poly(DT2,2) dry and wet.

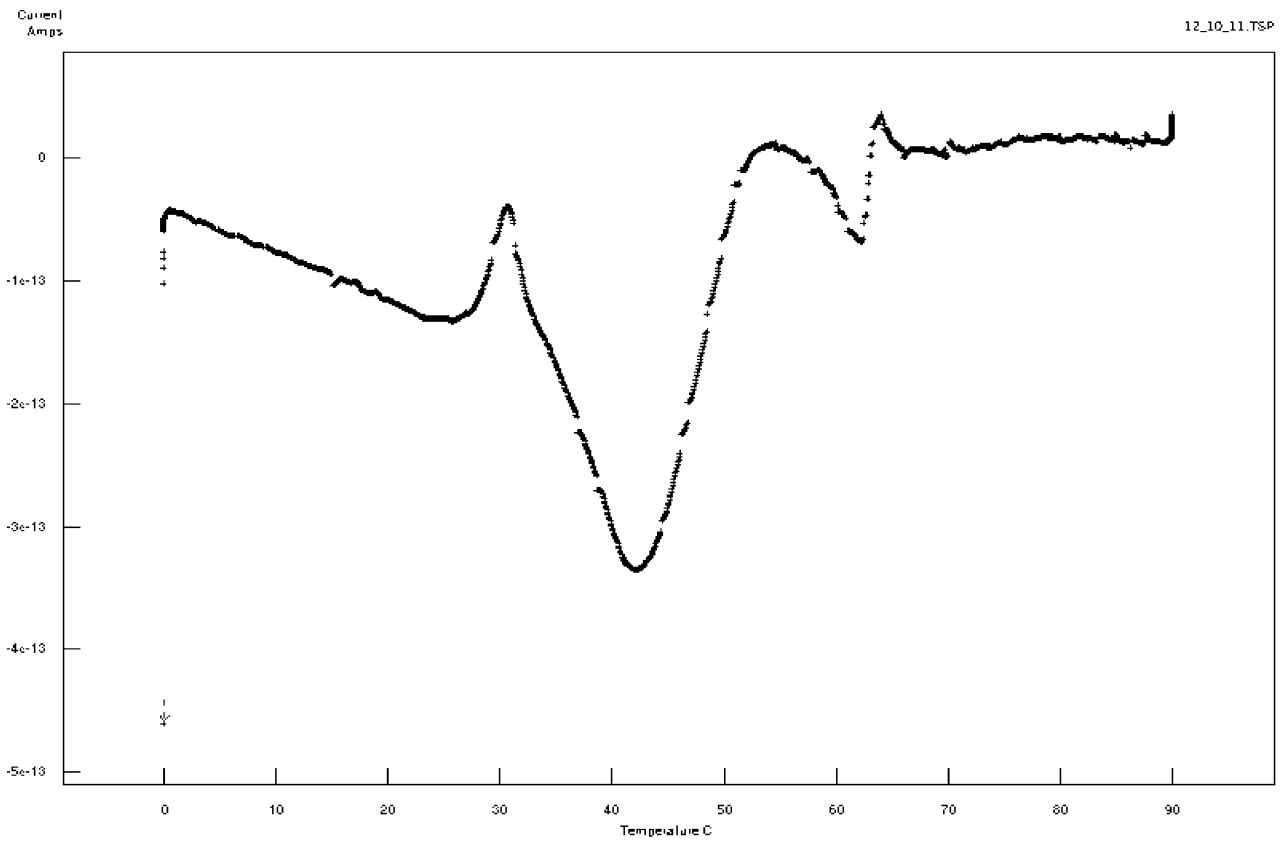

Fig. 7. Thermally stimulated current behavior of poly(DT12,10).

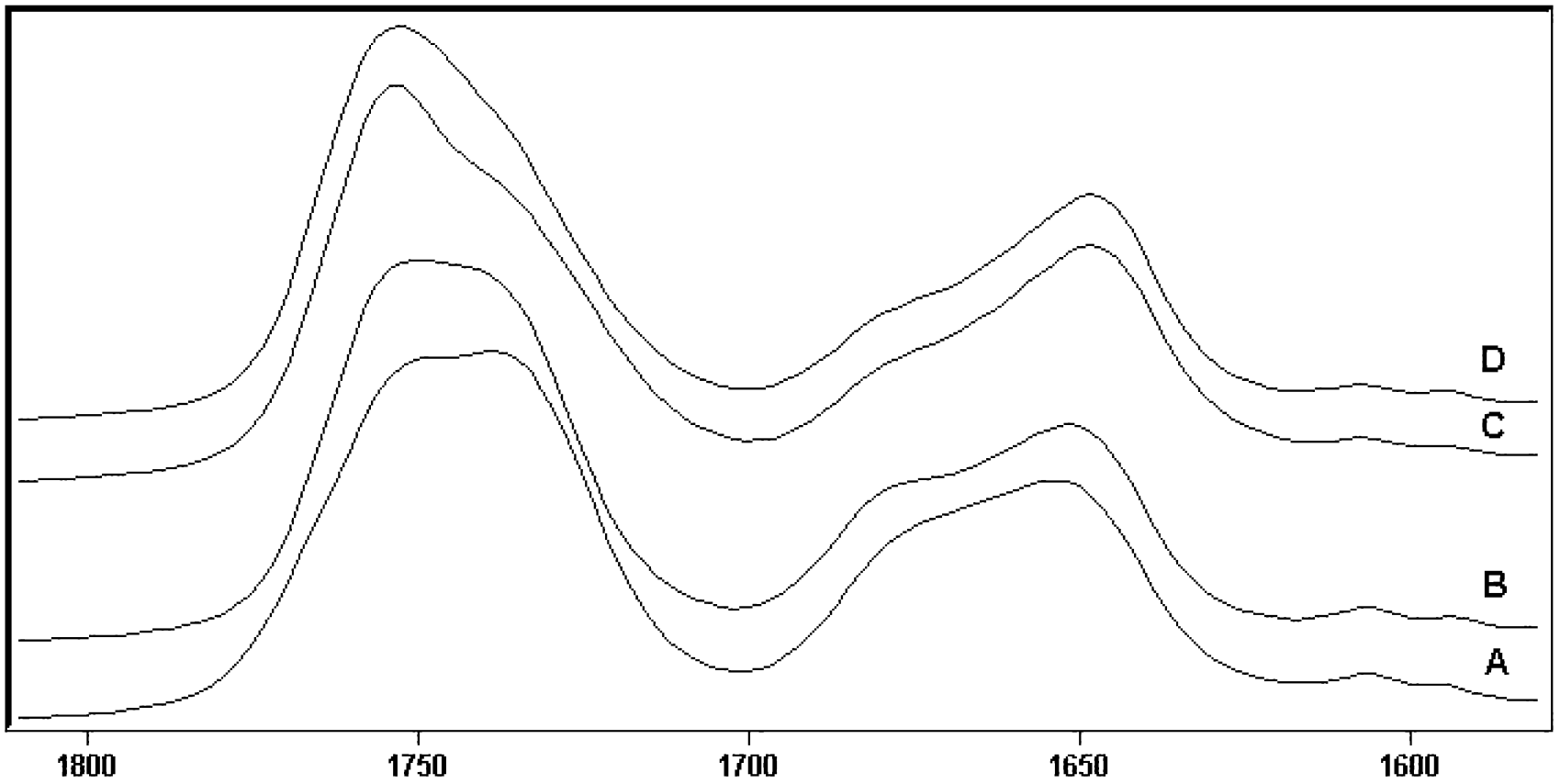

Fig. 8. Infrared spectra in C=O region (A) poly(DT2,2), (B) poly(DT2,10), (C) poly(DT8,8) and (D) poly(DT12,10).

also exhibit the free amide carbonyl bands near 1680 cm^{-1} and other bands near 1644 cm^{-1}. The hydrogen bonded carbonyl band has shifted to lower frequency for these ordered polymers, but two distinct bands for ordered and disordered hydrogen bonded carbonyls cannot be resolved. Evidence will be provided in a latter section for the existence of both these types of hydrogen bonded amide carbonyl species.

There are two structurally unique esters in these polymers. The main chain ester is an aryl/alkyl ester with the ester oxygen bonded to the aromatic ring whereas the side chain ester is an alkyl/alkyl ester. Therefore, one would expect two ester carbonyl bands with the higher frequency band associated with the main chain ester. However, more complex ester carbonyl band envelopes can also arise from conformational differences between amorphous and ordered phases [12] and from hydrogen bonded ester carbonyls [13]. The ester carbonyl band envelopes in the spectra of the four polymers are quite complex, but again these spectral components of the ordered and amorphous polymers can be easily distinguished from one another (Fig. 8). A more detailed elucidation of the nature of these bands will be given below where additional information derived from their thermal responses is provided and utilized for their assignments.

The infrared spectra of the four polymers investigated were obtained as a function of temperature between 25 and 100 °C in both heating and cooling modes. The poly(DT12,10) and poly(DT8,8) exhibited sharp spectral changes that corresponded to either phase change or phase formation phenomena, whereas the data for the other two polymers showed only continuous intensity variations related to temperature effects. Fig. 9 dramatically illustrates the spectral changes resulting from the transition at 41 °C upon cooling of the poly(DT12,10) polymer. There is a rapid drop in intensity of the band near 1644 cm^{-1} and an increase in intensity of the band near 1680 cm^{-1}. Furthermore, a band at 1652 cm^{-1} becomes visible. Similar sharp intensity changes denoting the transition are also easily observed for the poly(DT8,8) upon heating at 37 °C in Fig. 10 where the intensities of the 1644 and 1680 cm^{-1} bands are plotted versus temperature. The heating transition for the poly(12,10) was observed at 54 °C using this graphical procedure. These observations strongly suggest that three types of amides are present. Bands near 1680, 1652, and 1644 cm^{-1} can be assigned to free amide carbonyls, disordered hydrogen bonded amide carbonyls, and ordered hydrogen bonded amide carbonyls, respectively.

Upon cooling the poly(DT12,10), the 1644 cm^{-1} peak reappeared and the 1680 cm^{-1} band decreased below the transition temperature. However, no transition occurs when the poly(DT8,8) is cooled to room temperature and there is very little change in the appearance of the spectrum. The spectrum looks similar to the data for the amorphous form of these polymers. If the material is heated shortly after the cooling cycle, no phase change is detected. However, after standing for several days after cooling, the spectrum changes and is similar to the room temperature spectrum of the poly(DT12,10). A sample with this heat history will show a phase change transition again.

Analyzing samples that exist as pure amorphous or ordered materials at the same temperature provides an opportunity to spectrally isolate infrared bands associated with amorphous and ordered phases. These comparisons can be made for the poly(DT8,8) at room temperature with the heat treatments described above or for the poly(DT12,10) between the spectra obtained on heating and cooling between 41 and 54 °C. Fig. 11 displays spectra of amorphous and ordered poly(DT12,10) at 43 °C. All of the data are plotted on the same absolute intensity scale. A subtraction of the amorphous spectrum from the ordered spectrum reveals the bands related to the ordered phase. As is expected, the ordered hydrogen bonded amide carbonyl band is specifically related to the ordered phase.

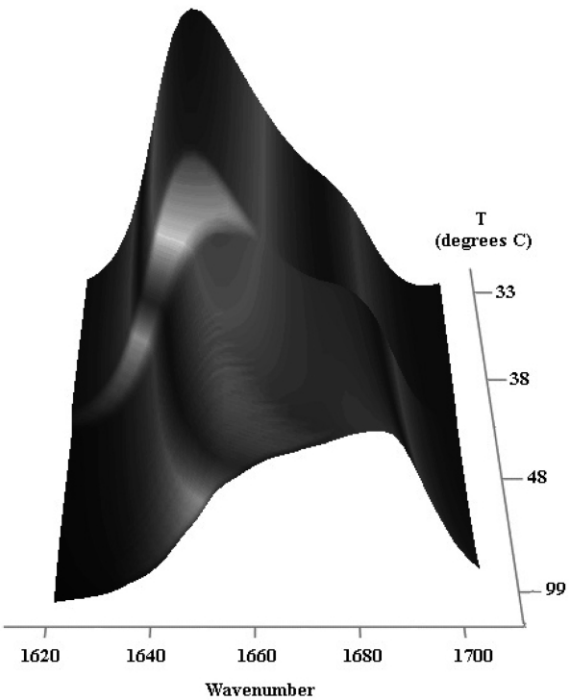

Fig. 9. Infrared spectra of the amide bands in poly(DT12,10) as a function of cooling.

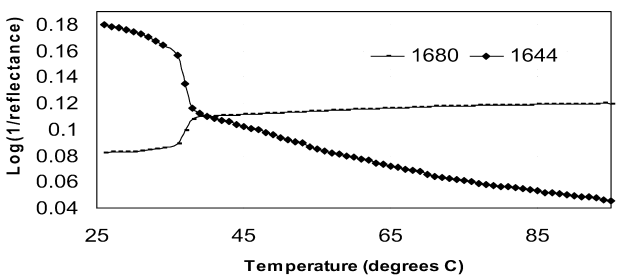

Fig. 10. Infrared intensities at 1680 and 1644 cm^{-1} as a function of heating—poly(DT8,8).

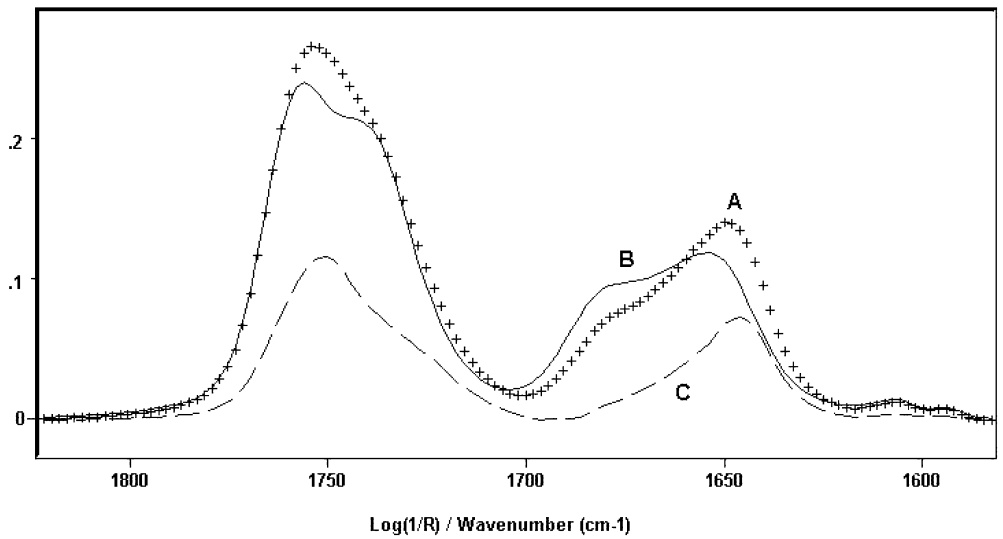

Fig. 11. Infrared spectra of poly(DT12,10) at 43 °C (A) Heating, (B) Cooling, (C) A–B.

There are also distinct changes in the ester band envelopes in the spectra of the poly(DT12,10) and poly(DT8,8) at their transition temperatures. This can be seen in Fig. 12 in the spectra of the poly(DT12,10) as it goes through its transition upon cooling. Two more or less distinct peak shapes at 1759 and 1740 cm^{-1} are replaced by a broader less resolved feature below 41 °C. Using the subtraction technique described above and illustrated in Fig. 11, specific ester frequencies can be associated with the ordered and amorphous phases. For the poly(DT12,10) bands at 1759 and 1740 cm^{-1} can be attributed to amorphous phase whereas peaks at 1752 and 1730 cm^{-1} are associated with the ordered phase. Similar results were obtained for the poly(DT8,8). The amorphous and ordered bands are 1758 and 1738 cm^{-1}, 1753 and 1728 cm^{-1}, respectively. The downward shifts in frequencies of the both the main and side chain esters in going from the amorphous phases to the ordered phases may suggest that there is some degree of hydrogen bonding of the esters in the ordered phases. These shifts may also be related to conformational differences between amorphous and ordered phases. A frequency difference of 18 cm^{-1} has been observed between the crystalline and amorphous carbonyl ester bands of poly(hydroxybutyrate) [13].

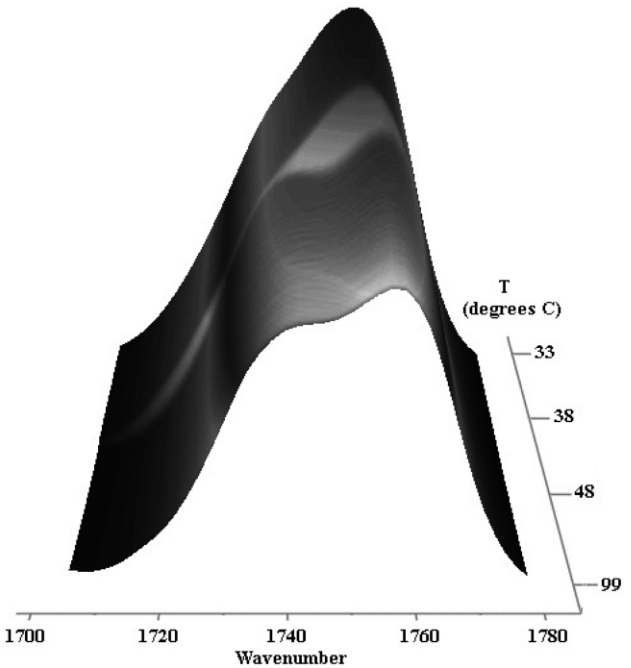

Fig. 12. Infrared spectra of the ester bands in poly(DT12,10) as a function of cooling.

Examination of the N–H stretching region may provide additional information about the possible hydrogen bonding to the ester carbonyls. Fig. 13 displays the spectra of the four polymers in the N–H stretching region. The bands are similar to those found in the spectra of copolyesteramides of ϵ-caprolactam with ϵ-caprolactone [14–17] and hexamethylene adipamide with hexamethylene adipate [15]. According to the literature, bands near 3300, 3380, 3430 (shoulder), and 3495 cm^{-1} can be assigned to N–H bonded to amide carbonyls [7,8], N–H bonded to ester carbonyls [14–16], free N–H and/or the overtones of the side chain esters, and the overtones of the main chain ester, respectively. Therefore, the presence of 3380 cm^{-1} bands in the spectra strongly suggests that there is N–H bonding to ester carbonyls.

Analysis of the N–H region as the material goes through the transition provides significant insight into nature of the hydrogen bonding in the ordered and amorphous phases. Fig. 14 displays data extracted from the cooling experiments for the poly(DT12,10). Spectra ‘B’ and ‘A’ were recorded at 43 and 39 °C, respectively. The transition occurs at 41 °C. This region of both spectra was also analyzed with curve fitting utilizing five bands, described above, in the fits. The primary amide N–H bonding peak near 3300 cm^{-1} increased approximately twenty five percent when the

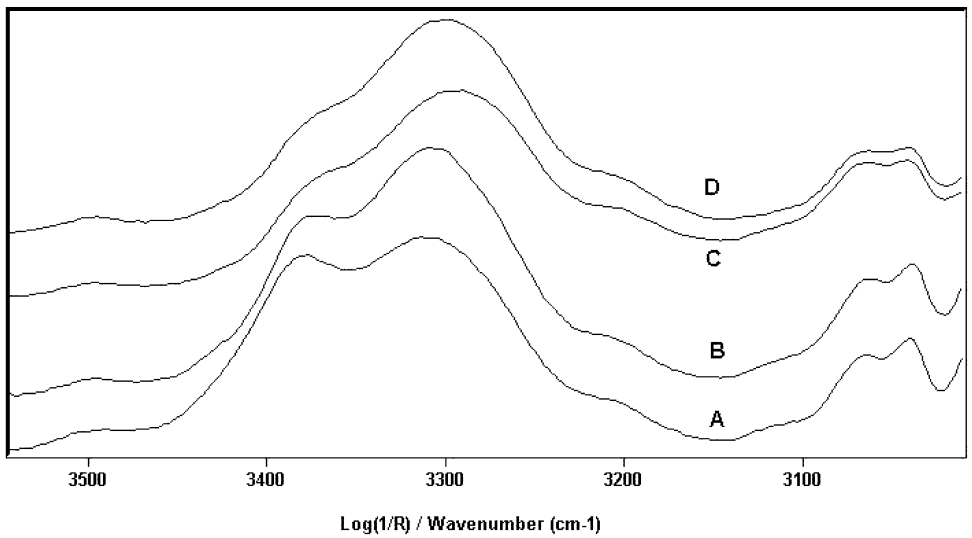

Fig. 13. Infrared spectra in the N–H region (A) poly(DT2,2), (B) poly(DT2,10), (C) poly(DT8,8), and (D) poly(DT12,10).

ordered phase was formed. This is consistent with the formation of the stronger hydrogen bonds as evidenced by the appearance of the 1644 cm^{-1} amide carbonyl band. However, the intensity of the band near 3380 cm^{-1} is nearly constant for the spectra at both temperatures. This result suggests that the hydrogen bonding to the esters is the same above and below the transition, which implies that the hydrogen bonded esters are associated with the amorphous phase or that there are disordered H bonds trapped within the ordered phase. If this is correct, then the two sets of ester carbonyls, for the poly(DT12,10) (1759 and 1740 cm^{-1}) and 1752 and 1730 cm^{-1}), can be attributed to differences in the conformations of non-hydrogen bonded esters in the amorphous and ordered phases. Furthermore, the ester carbonyl band envelopes must contain some weak unresolved components that are associated with hydrogen bonded esters.

4. Conclusions

It has been clearly shown that the long range ordered phase noted in poly(DT12,10) and poly(DT8,8) is associated with ordered H bonds in the N–H region. While a combination of infrared, thermal analysis optical microscopy and X-ray diffraction data, suggest that the mesogenic structures observed are best described as smectic-like or ‘condis’, the assignment of phase is less important than the impact the presence of the phase on in vivo performance. Wide-angle X-ray diffraction results indicate that there is a single spacing along the meridian, corresponding to about 2.7 nm, about the distance between amide linkages or between side-chains along the backbone. The heating and cooling infra-red data shown in Figs. 9–12, when combined with the thermal analysis (Figs. 3 and 7, also see Refs. [3,4]) show unequivocally that the formation of

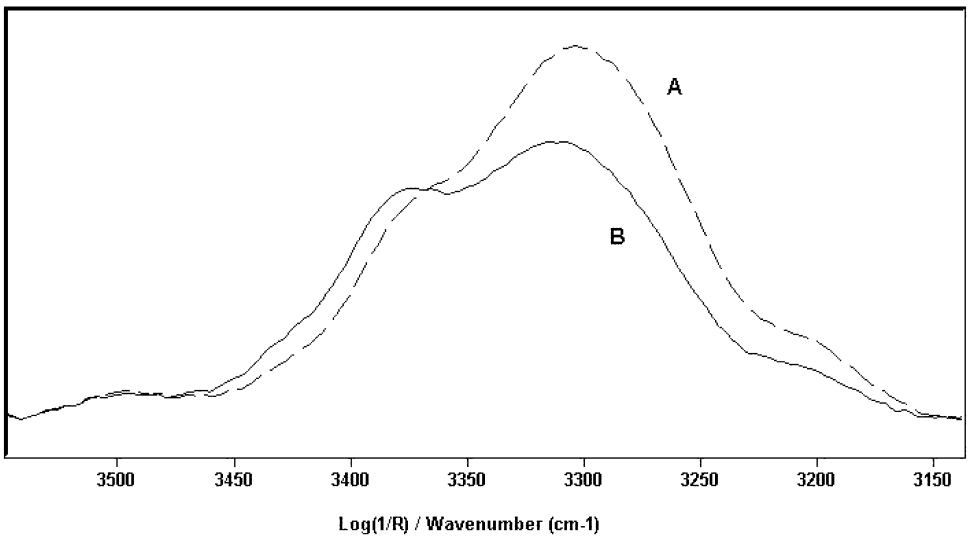

Fig. 14. Infrared spectra in the N–H region of poly(DT12,10)—(A) 39 °C, (B) 43 °C (data extracted from cooling run).

ordered H bonds and the formation or the destruction of the long range order is linked Without further information or examination of other polymer compositions it is not possible to positively identify the chemical entity along the molecular backbone reflected in the layer spacing observed in the wide angle X-ray diffraction data, although it is likely that the smectic-like order is associated with the H-bond spacing. It is also likely that the side-chains (of a similar length to the noted repeat distance) are packed parallel to the molecular backbone rather than normal to it. The X-ray diffraction data show no indication that a similar repeat distance, related to the sidechain length, exists transverse to the molecular backbone. Disordered H bonds can also be found in compositions that exhibit long-range order. The terms ordered and disordered hydrogen bonds relate to the strength and distance associated with a given H-bond, i.e. ordered bonds are stronger than disordered bonds. These effects are associated with molecular packing in materials that allow these close interactions to occur. The compositions investigated that do not exhibit long range order, i.e. the compositions that exhibit only amorphous structure (poly(DT2,2) and poly(DT2,10)) contain only disordered H bonds in the N–H region. Heating and cooling experiments show unequivocally that the formation of order in these polymers is related to the nature of the H bonding. It is not clear, however, whether the long-range order is caused or stabilized by strong H-bond formation. A consequence of the ordered H bonds is the resistance of these compositions to plasticization by water [3,4], vital for the retention of process induced structure and lack of shrinkage under biorelevant conditions.

There is also some hydrogen bonding observed between the amide N–H and ester carbonyls. However, this bonding is found only in the amorphous phase. There are also conformational differences between the non-hydrogen bonded ester carbonyls in the ordered and amorphous phases. The variation most likely results from the presence or lack of structural alignments imposed by the amide-amide hydrogen bonding in the ordered and amorphous phases.

Given the equal possibility of head to head or head to tail polymerization of the asymmetric DT monomer into the chain backbone within the poly(DTR,Y) combinatorial library, and the need for antiparallel packing for the chain to chain H-bonds to form in the N–H region it would be expected that not all N–H moieties along the chain would be able to form ordered H bonds. Once the ordered H bonds were formed, both disordered H bonds and unassociated carbonyls would be distributed throughout the structure. It is unclear whether these would be trapped within a global mesogenic structure or phase separate into a distinct amorphous phase. Most of the information gathered in this work suggests that the smectic like structure is global—lack of molecular relaxation at T_g, no evidence of separate phases in optical microscopy. It is clear that upon heating of the poly(DT8,8) and the poly(DT12,10) to above the critical transition temperatures the ordered H-bonds disappear while the disordered H-bonds persist. Under these conditions there is no difference in behavior between any of the four polymer compositions investigated.

While mesogenicity and partitioning of H bonds energies have been previously observed in ester-amide polymers [11–13,15], the richness of structure observed here was unanticipated. Definition of the range of compositions that exhibit the ordering observed in this study as well as the ability to translate these results to other backbone chemistries remain ongoing research questions. The value of forming long-range ordered structures in erodable polymeric biomaterials is evidenced in the retention of mechanical properties and heightened dimensional stability under in vivo use conditions [3,4]. Effects of differing H-bonding regimes on the binding of proteins to these materials and the subsequent response of cells to these surfaces are currently under investigation.

Acknowledgements

The authors thank Professor Joachim Kohn of Rutgers University for his discussions and insights during the progress of this work. The contributions of Professor J. Wu in obtaining and analyzing the X-ray diffract results is appreciated. Discussions with Professor Michael Dunn of the Robert Wood Johnson Medical School and Dr Sharon Bourke of Rutgers University are gratefully acknowledged. Support for this work from the New Jersey Center for Biomaterials, the National Institutes of Health and the NIH—National Institute for Biomedical Imaging and Bioengineering, P41 EB 000922-01 is recognized with thanks.

References

[1] Griffin LG. Acta Materialia 2000;48(1):263–77.
[2] Rimmer S. Special Publ R Soc Chem 2001;263:89–99.
[3] Jaffe M, Ophir Z, Pai V. Thermochim Acta 2003;396:141–52.
[4] Jaffe M, Pai V, Ophir Z, Wu J, Kohn J. Polym Adv Technol 2002;13:926–37.
[5] Brocchini S, James K, Tangpasuthadol V, Kohn J. J Am Chem Soc 1997;119:4553–4.
[6] Kohn J, Brocchini S, James K, Tangpasuthadol V. Book of Abstract, 217th ACS National Meeting, 1999, POLY-178.
[7] Jaffe M, Warner SB. Quiescent crystallization in thermotropic polymers. J Cryst Growth 1980;48:184.
[8] Wunderlich BW, Moeller M, Grebowicz J, Baur H. Adv Polym Sci 1988;87:1–121.
[9] Wunderlich BW. Thermochim Acta 1999;340–341:37–52.
[10] Skrovanek D, Howe SE, Painter PC, Coleman MM. Macromolecules 1985;18:1676.
[11] Skrovanek D, Painter PC, Coleman MM. Macromolecules 1986;19:699.
[12] Iriondo P, Iruin JJ, Fernandez-Berridi MJ. Polymer 1995;36:3235.
[13] Goodman A. Valavanidis. Eur Polym J 1984;20:241.
[14] Goodman RN. Vachon. Eur Polym J 1984;20:529.
[15] Goodman. Eur Polym J 1984;20:549.
[16] Goodman RJ. Sheahan. Eur Polym J 1990;26:1089.
[17] Kaczmarczyk B. Polymer 1998;39:5853.